Characterization of Spo11-dependent and independent phospho-H2AX foci during meiotic prophase I in the male mouse

Alexandre Chicheportiche, J. Bernardino-Sgherri, Bernard de Massy, B. Dutrillaux

Characterization of *Spo11*-dependent and independent phospho-H2AX foci during meiotic prophase I in the male mouse

Alexandra Chicheportiche[1,2,3,*], Jacqueline Bernardino-Sgherri[1,2,3], Bernard de Massy[4] and Bernard Dutrillaux[5]

[1]Laboratory of Differentiation and Radiobiology of the Gonads, Unit of Gametogenesis and Genotoxicity, Unité Mixte de Recherche-S 566, Commissariat à l'Energie Atomique DSV/IRCM/SEGG/LDRG, F-92265 Fontenay aux Roses, France
[2]Université Denis Diderot Paris 7 and [3]Institut National de la Santé et de la Recherche Médicale, Unité 566, F-92265 Fontenay aux Roses, France
[4]Human Genetic Institut, CNRS UPR 1142, 141 rue de la Cardonille 34396 Montpellier Cedex 5, France
[5]National Museum of Natural History, CNRS UMR 5202, 16 rue Buffon, 75005 Paris, France
*Author for correspondence (e-mail: alexandra.chicheportiche@cea.fr)

Accepted 20 March 2007
Journal of Cell Science 120, 1733-1742 Published by The Company of Biologists 2007
doi:10.1242/jcs.004945

Summary

Meiotic DNA double strand breaks (DSBs) are indicated at leptotene by the phosphorylated form of histone H2AX (γ-H2AX). In contrast to previous studies, we identified on both zygotene and pachytene chromosomes two distinct types of γ-H2AX foci: multiple small (S) foci located along autosomal synaptonemal complexes (SCs) and larger signals on chromatin loops (L-foci). The S-foci number gradually declined throughout pachytene, in parallel with the repair of DSBs monitored by repair proteins suggesting that S-foci mark DSB repair events. We validated this interpretation by showing the absence of S-foci in *Spo11*$^{-/-}$ spermatocytes. By contrast, the L-foci number was very low through pachytene. Based on the analysis of γ-H2AX labeling after irradiation of spermatocytes, the formation of DSBs clearly induced L-foci formation. Upon DSB repair, these foci appear to be processed and lead to the above mentioned S-foci. The presence of L-foci in wild-type pachytene and diplotene could therefore reflect delayed or unregulated DSB repair events. Interestingly, their distribution was different in *Spo11*$^{+/-}$ spermatocytes compared with *Spo11*$^{+/+}$ spermatocytes, where DSB repair might be differently regulated as a response to homeostatic control of crossing-over. The presence of these L-foci in *Spo11*$^{-/-}$ spermatocytes raises the interesting possibility of yet uncharacterized alterations in DNA or chromosome structure in *Spo11*$^{-/-}$ cells.

Key words: γ-H2AX, Meiosis, DNA double strand breaks, *Spo11*

Introduction

Meiosis is a specialized form of cell division essential to generate gametes in sexually reproducing organisms. Following a single round of DNA replication, two successive rounds of chromosome segregation lead to haploid gametes. Meiotic recombination is required to sort the two sets of homologs and connect the corresponding chromosome pairs, so that they can segregate accurately at meiosis I. In almost all species, meiotic prophase is characterized by the formation of programmed DSBs catalyzed by the SPO11 protein, which triggers the initiation of homologous recombination. In *Spo11*-deficient mice, spermatocytes are eliminated by apoptosis at late zygotene/early pachytene as a consequence of chromosome structural defects or synaptic failures (Baudat et al., 2001; Romanienko et al., 2000).

The events that proceed from SPO11-induced DSBs are not yet fully elucidated in mammals but have been extensively characterized in yeast. Studies in *S. cerevisiae* have shown that a complex regulation operates in order to channel recombination events via the classical DSB repair (Szostak et al., 1983) or via synthesis-dependent strand annealing (SDSA) into at least two outcomes: (1) crossover (CR), the reciprocal product of recombination between homologous chromosomes and (2) gene conversion without CR (NCR) (Allers et al., 2001; Borner et al., 2004; de los Santos et al., 2003). In mouse, the number of DSBs was estimated on the basis of the cytological detection of RAD51/DMC1 proteins, which are thought to represent early intermediates of recombination (Ashley et al., 1995; Barlow et al., 1997; Moens et al., 1997). Both proteins catalyze the invasion and strand-exchange reaction between homologous chromosomes forming joint molecules. They appear in high abundance after DNA breakage, i.e. at leptotene. In the male, their number peaks at about 300 foci per nucleus and gradually declines from 200 to 100 foci during zygotene to disappear completely at diplotene. Almost all RAD51 and DMC1 foci colocalize on chromosomes during the successive stages of the meiotic prophase (Moens et al., 2002; Tarsounas et al., 1999). CRs are cytologically identified by the presence of the mismatch repair protein homologs MLH1 and MLH3: both colocalize on chromosome axes of pachytene bivalents (Anderson et al., 1999; Baker et al., 1996; Lipkin et al., 2002; Marcon et al., 2003). Number and distribution of these specific events of recombination, on average 23 per mouse spermatocyte, are controlled so that each chromosome undergoes at least one CR that will become visible as chiasma at diplotene/diakinesis. Analysis of meiotic recombination has also been performed by molecular detection of gene-conversion events repair, throughout the first wave of spermatogenesis (Guillon et al., 2002).

H2AX, a highly conserved histone H2A variant, accounts

for 10-20% of the total H2A proteins of chromatin (Redon et al., 2002). It is found in large amounts in adult germ cells (Nagata et al., 1991; Tadokoro et al., 2003; Yoshida et al., 2003). H2AX differs from other H2A isoforms by the presence of a conserved SQ motif at the C-terminus that is phosphorylated on the serine residue 139 in mammals. Its modified form, named γ-H2AX (Rogakou et al., 1998), rapidly appears after DSB induction in the form of nuclear foci that contain proteins involved in both DNA repair (Paull et al., 2000) and checkpoint signaling (Bassing et al., 2004; Peterson et al., 2004). In cultured mammalian somatic cells, appearance of γ-H2AX foci peaks within 30-60 minutes following exposure to radiation (IR) (MacPhail et al., 2003; Rogakou et al., 1999; Rogakou et al., 1998). Each focus corresponds to one DSB (Sedelnikova et al., 2002). The wave of H2AX phosphorylation spreads several DNA megabases from each side of the break and promotes structural chromosome changes. The chromatin remodeling serves to concentrate and retain factors in the vicinity of the lesion, and helps to keep ends tethered together (Bassing et al., 2004; Fernandez-Capetillo et al., 2004; Thiriet et al., 2005).

In male mouse spermatocytes γ-H2AX is spatially and temporally linked to synapsis and meiotic DSBs (Mahadevaiah et al., 2001). During leptotene, it is abundant and encompasses a large proportion of the developing axial elements containing DMC1 foci that are *Spo11*-dependent (Baudat et al., 2000; Romanienko et al., 2000). Throughout zygotene, DMC1 foci on asynapsed region of axial elements continue to be located within γ-H2AX domains. Once autosomal synapsis has occurred γ-H2AX is found to be restricted to the XY chromatin and non-synapsed autosomal regions (Mahadevaiah et al., 2001), just prior to meiotic sex chromosome inactivation (MSCI) and meiotic silencing of unsynapsed chromatin (MSUC) (Mahadevaiah et al., 2001; Turner et al., 2005; Baarends et al., 2005). Phosphorylation of H2AX specifically associated with the XY body has been shown to be driven by ATR via BRCA1 to asynapsed chromatin (Baart et al., 2000; Turner et al., 2004) and is also dependent on *Spo11* (Bellani et al., 2005). The repair of SPO11-induced DSBs lasts 7 days in mice and can be monitored by the immunolocalization of repair proteins, such as RAD51, RPA or MSH4, on pachytene spermatocyte spreads (Moens et al., 2002; Neyton et al., 2004). Interestingly, several studies on somatic cells showed that the kinetics of γ-H2AX loss is related to DNA repair activity (Nazarov et al., 2003; Rothkamm et al., 2003), but completion of DSB repair does not necessarily imply the disappearance of γ-H2AX foci (Antonelli et al., 2005; Bouquet et al., 2006; Forand et al., 2004). Thus, because γ-H2AX foci on synaptonemal complexes (SCs) are markers of SPO11-dependent DSB repair at early stages of the meiotic prophase (Hunter et al., 2001; Mahadevaiah et al., 2001), they might still be detectable at pachytene. Accordingly, γ-H2AX foci were detected along SCs in human and grasshopper pachytene cells, and colocalized with repair protein foci (Lenzi et al., 2005; Roig et al., 2004; Viera et al., 2004). By contrast, no γ-H2AX foci were observed at this stage in mouse spermatocytes by Mahadevaiah et al. (Mahadevaiah et al., 2001), suggesting differences between species in the dynamics of H2AX phosphorylation/dephosphorylation (Lenzi et al., 2005). We have reexamined the phosphorylation of H2AX on mouse spermatocytes and observed two types of foci that are present at the pachytene stage but have distinct kinetics and functional properties. We propose that small (S) γ-H2AX foci (S-foci) specifically indicate sites of SPO11-DSBs undergoing repair, wheras larger γ-H2AX signals on chromatin loops (L-foci) target both unrepaired SPO11-DSBs and SPO11-independent events.

Results

Distinct γ-H2AX signals are associated with spermatocyte chromosomes

Mahadevaiah et al. have previously described the expression of γ-H2AX during prophase I in mice by using immunofluorescence (Mahadevaiah et al., 2001). This expression was defined as γ-H2AX domains at leptotene and zygotene stages whose intensity declined on autosomes in relation with synapsis formation. Then, from late zygotene to diplotene γ-H2AX staining exclusively involved the sex body. Functionally, the first wave of H2AX phosphorylation is thought to represent the response to the SPO11-dependent formation of meiotic DSB, whereas the second wave is related to MSCI. When we monitored H2AX phosphorylation in late zygotene to pachytene stages we found, apart from the sex body staining, two distinct types of relatively weak γ-H2AX signal: S foci that are located on the SC and also L-foci, the broader signals that are linked to the SC protrude along chromatin loops (Fig. 1Aa,b,e,f).

S-foci have properties compatible with sites of meiotic DSB repair

To assess a possible relationship between these γ-H2AX foci and meiotic DSBs, we first quantified the time course of both γ-H2AX foci. At zygotene, the number of γ-H2AX foci was too high to be quantified with confidence (Fig. 1Aa). At pachytene, although the intense labeling of sex chromosomes generally overlapped with one or more SCs, we found an average of 120 S-foci per cell at early pachytene (Table 1, Fig. 1Ab). This number was fairly constant from cell to cell and mouse to mouse. However, differences were observed according to mouse strains, age and rodent species (Table 1). For instance, greater numbers of S-foci per cell were found in juvenile compared with adult mice; S-foci number also varied in a way that was independent of the number of bivalents in guinea pig and chinchilla (Table 1, Fig. 1Ac,d). At late pachytene, the number of S-foci per cell decreased to 48 (n=78 cells, 2.55±1.17 per bivalent, Fig. 1Ae). No S-foci were seen at diplotene (Fig. 1Af).

By contrast, L-foci were much less frequent at both early (Table 1) and late (1.64±1.64 per cell, n=86 cells) pachytene stages. However, their distribution in early- and late-pachytene cells was completely different (χ^2>13.82, υ=2, P<0.001) (Fig. 1B). Indeed, from early to late pachytene we observed the accumulation of cells containing more than two L-foci (14% to 47%, respectively). L-foci were still observed at diplotene in the same proportion as at pachytene (0.67±0.9 per cell, P>0.05, n=50 cells). Notice that, even at diakinesis the mean number of γ-H2AX signals remained constant (1.12±1.86, P>0.05, n=84). However, we found that the distribution of cells according to the number of L-foci was different between late pachytene and diplotene (χ^2=11.7, υ=2, P=0.003) (Fig. 1B). The proportion of cells devoid of L-foci increased from

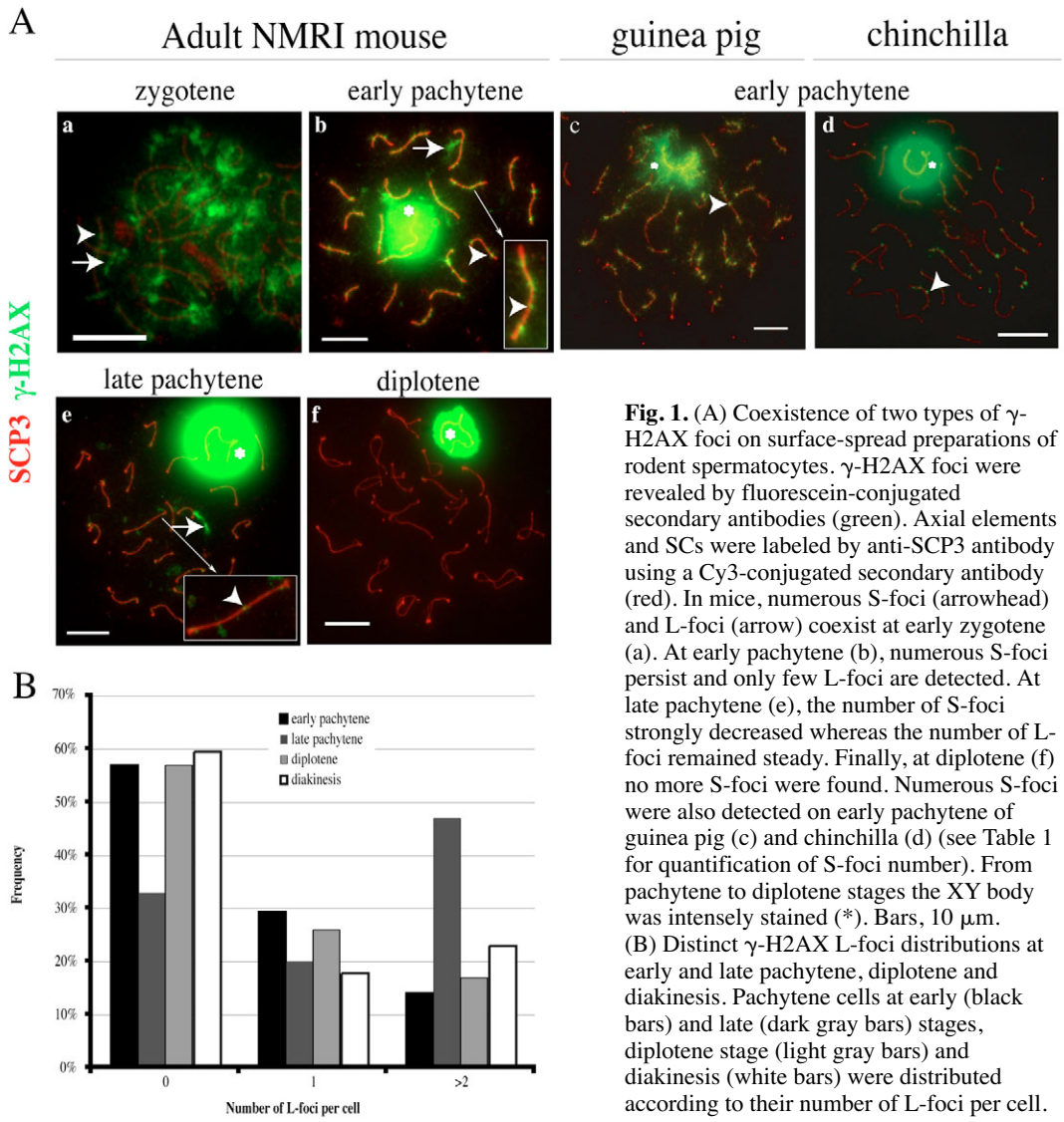

Fig. 1. (A) Coexistence of two types of γ-H2AX foci on surface-spread preparations of rodent spermatocytes. γ-H2AX foci were revealed by fluorescein-conjugated secondary antibodies (green). Axial elements and SCs were labeled by anti-SCP3 antibody using a Cy3-conjugated secondary antibody (red). In mice, numerous S-foci (arrowhead) and L-foci (arrow) coexist at early zygotene (a). At early pachytene (b), numerous S-foci persist and only few L-foci are detected. At late pachytene (e), the number of S-foci strongly decreased whereas the number of L-foci remained steady. Finally, at diplotene (f) no more S-foci were found. Numerous S-foci were also detected on early pachytene of guinea pig (c) and chinchilla (d) (see Table 1 for quantification of S-foci number). From pachytene to diplotene stages the XY body was intensely stained (*). Bars, 10 μm. (B) Distinct γ-H2AX L-foci distributions at early and late pachytene, diplotene and diakinesis. Pachytene cells at early (black bars) and late (dark gray bars) stages, diplotene stage (light gray bars) and diakinesis (white bars) were distributed according to their number of L-foci per cell.

late pachytene (33%) to diplotene (57%) giving evidence of DSB repair and/or cell elimination.

To check whether S- and L-foci correspond to sites of DSB undergoing repair, we looked for their possible colocalization with RAD51/DMC1 foci at early/mid-pachytene (Fig. 2Aa). Ten cells at early/mid-pachytene were analyzed and the proportions of either RAD51 or γ-H2AX foci versus mixed foci were calculated. Among the 230 RAD51 foci recorded, 57% colocalized with one of the 1100 γ-H2AX S-foci, a further 13% were neighboring with γ-H2AX S-foci.

At late pachytene, about 50 S-foci were still present on SCs. In agreement with published data (Anderson et al., 1999;

Table 1. Average numbers of γ-H2AX S- and L-foci ± s.d. in early pachytene spermatocytes from mice, Guinea pig and chinchilla

	Mean number of γ-H2AX S-foci ± s.d. per bivalent	Number of bivalents	Number of analysed cells (animal number)	Mean number of γ-H2AX L-foci ± s.d. per cell	Number of analysed cells (animal number)	Statistics
Mouse NMRI (15 dpp)	7.59±2.02	19	70 (3)	1.40±1.68	68 (3)	$^{*}P<0.01$ $^{\dagger}P>0.05$
Spo11+/+ mouse C57BL6/129SvJ (15 dpp)	7.63±1.73	19	72 (3)	1.26±1.38	72 (3)	$^{*}P<0.05$
Mouse NMRI (adult)	6.28±1.15	19	120 (3)	0.772±1.27	57 (3)	$^{\ddagger}P<0.05$
Mouse C57BL6/129SvJ (adult)	7.03±1.04	19	43 (2)	1.18±1.12	40 (2)	–
Guinea pig	5.29±1.01	31	25 (2)	–	–	–
Chinchilla	3.13±0.70	31	36 (1)	–	–	–

Data from all experiments were pooled to calculate the mean numbers and standard deviation (s.d.). Mann-Whitney U-test was used to compare the S-foci number per bivalent of juveniles and adults (*), juvenile mouse strains (†) and adult mouse strains (‡). dpp, days post partum.

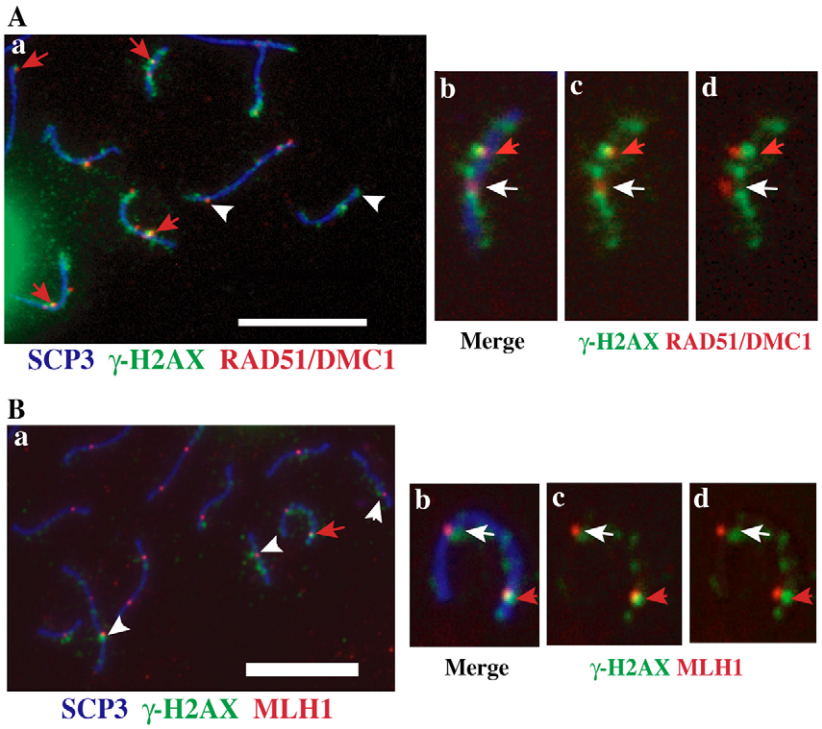

Fig. 2. (A) γ-H2AX-containing S-foci partially colocalize with RAD51 foci on SCs. (a) Partial mid-pachytene chromosome spread stained with anti-γ-H2AX (green), anti-RAD51 (red) and anti-SCP3 (blue) antibodies. Examples of non-colocalized γ-H2AX and RAD51 foci are indicated by white arrowheads. Mixed γ-H2AX/RAD51 foci are marked by red arrows. (b-c) Higher magnification of one synapsed chromosome core (b) triple-labeled with anti-γ-H2AX (green), anti-RAD51 (red) and anti-SCP3 (blue) antibodies, (c) double-labeled with anti-γ-H2AX, and anti-RAD51 are shown. γ-H2AX and RAD51 foci are slightly offset to show their colocalization more clearly (d). Red and white arrows indicate sites of colocalized and juxtaposed foci, respectively. (B) γ-H2AX S-foci partially colocalize with MLH1 foci on SCs. (a) Partial pachytene chromosome spread stained with anti-γ-H2AX (green), anti-MLH1 (red) and anti-SCP3 (blue) antibodies. Examples of non-colocalized γ-H2AX and MLH1 foci are indicated by white arrowheads. The only mixed focus on this image is indicated by a red arrow. (b-d) Enlarged images of one SC triple-labeled with (b) anti-γ-H2AX (green), anti-MLH1 (red) and anti-SCP3 (blue) antibodies, and (c) double-labeled with anti-γ-H2AX and anti-MLH1 antibodies. (d) γ-H2AX and MLH1 foci are slightly offset. White arrows indicate juxtaposed foci; red arrows indicate colocalized foci. Bars, 10 μm.

Ashley et al., 2004), we observed that MLH1 foci appeared at mid-pachytene, their number reaching a maximum of 24.6±2.5 per cell (n=181). Among 26 spermatocyte nuclei, we recorded 529 MLH1-only foci, 1640 pure S-foci and 122 mixed MLH1–S-foci. Thus, mixed foci represented 19% of all MLH1 foci and an additional 25% of MLH1 foci were immediately neighboring one of the S-foci (Fig. 2Ba). We did not observe any colocalization of L foci with RAD51 or MLH1.

Spo11$^{-/-}$ zygotene spermatocytes display exclusively L-foci

If L- and S-foci in spermatocytes mark DSB formation and repair events, respectively, these foci were expected to be *Spo11* dependent. We therefore investigated γ-H2AX formation in *Spo11*$^{-/-}$ mice. In these mice, meiotic cells are arrested at the end of zygotene or the beginning of pachytene and are subsequently eliminated by apoptosis. We, therefore, focused our analysis on juvenile mice (15 days post partum) to avoid the analysis of apoptotic cells, which are more abundant in adult mice (Baudat et al., 2000). It is noteworthy that in nuclei of *Spo11*$^{-/-}$ spermatocytes a γ-H2AX domain is observed. Although it looks similar to a sex body, it was actually found not to colocalize with X or Y chromosomes (which are not synapsed in *Spo11*$^{-/-}$ mutants) and was therefore called the pseudo sex body (Barchi et al., 2005; Bellani et al., 2005).

In our analysis, no S-foci was detected in *Spo11*$^{-/-}$ zygotene/early pachytene spermatocytes, which is in agreement with our interpretation for a relationship between DSB repair and S-foci formation (compare Fig. 3Aa,b controls with 3Ac,d *Spo11*$^{-/-}$ cells). Surprisingly, we observed cells with γ-H2AX signals that looked like L-foci attached to the chromosome cores labeled by SCP3 staining (Fig. 3Ac). This was in addition to detecting the signal that corresponded to the pseudo sex body. In fact, we identified two categories of *Spo11*$^{-/-}$ nuclei – one with and one without the pseudo sex body (Fig. 3Ac,d) – predicted to correspond to early and late zygotene, respectively. This was indeed confirmed by co-labeling cells with SCP1 (a marker for the transversal element of the SC) and anti-γ-H2AX antibodies (Fig. 3Ac′,d′). We found that 24% of nuclei positive for SCP1 (12 nuclei, n=51) were devoid of pseudo sex bodies, whereas 76% (39 nuclei, n=51) did exhibit a pseudo sex body. These results are coherent with the fact that, upon progression into zygotene, non homologous synapsis proceeds while a pseudo sex body is formed (Fig. 3Ad,d′). We found a high number of L-foci in zygotene *Spo11*$^{-/-}$ cells (from 1 to 20). The number of L-foci per cell was significantly higher in early (8.33±3.78, n=58 cells) than in late zygotene stage (6.84±3.69, n=61 cells; P=0.02). We observed that the distribution of *Spo11*$^{-/-}$ nuclei, according to their number of L-foci, was not homogeneous at early zygotene (χ^2=8.35, υ=2, P=0.01) compared with late zygotene (χ^2=5.62, υ=2, P>0.05) (Fig. 3B). Namely, we found that the proportion of nuclei with more than ten L-foci was greater (38%) at early zygotene than at late zygotene (17%) (χ^2=5.76, υ=1, P=0.016). These results show that L-foci can occur in the absence of SPO11. The trigger involved is not known but could be related to synaptic failure or chromosome structure alterations. Whatever the mechanism, it is possible that L-foci formed in early zygotene are processed and clustered, then leading to the formation of the pseudo sex body at late zygotene.

γ-H2AX pattern in Spo11$^{+/-}$ pachytene spermatocytes

Given that *Spo11*$^{-/-}$ spermatocytes do not proceed to pachytene, we compared *Spo11*$^{+/-}$ and *Spo11*$^{+/+}$ spermatocytes for their γ-H2AX pattern at pachytene. We found the same

number of S-foci at early and late pachytene on *Spo11*$^{+/+}$ (7.63±1.73 per bivalent, *n*=72 cells; 3.66±1.50 per bivalent *n*=46 cells) and *Spo11*$^{+/-}$ (7.64±1.37 per bivalent *n*=81; 3.05±1.12 per bivalent *n*=40) spermatocytes (Fig. 4A). In contrast to S-foci, more L-foci were found in *Spo11*$^{+/-}$ (*n*=81 cells) than in *Spo11*$^{+/+}$ (*n*=72 cells) pachytene cells but the difference was only significative at early pachytene ($P<0.0001$; Fig. 4B). In addition, the distribution of the number of L-foci per cell during pachytene stage progression was the opposite in *Spo11*$^{+/+}$ *and Spo11*$^{+/-}$ cells ($\chi^2>18.4$, $\upsilon=2$, $P<0.0001$). In *Spo11*$^{+/+}$ cells, late pachytene had the highest number of L foci, whereas in *Spo11*$^{+/-}$ cells, early pachytene had the highest number of L foci (Fig. 4C).

Both S- and L-foci are induced by DSB inducers

To understand the potential relationship between L-foci and DSB-repair events, we analyzed the consequence of γ-irradiation of spermatocytes on the formation γ-H2AX foci. Mice were first exposed to γ-rays at increasing doses up to 2 Gy (Fig. 5A). Pachytene cells were analyzed 8 hours after irradiation to allow a reliable quantification of γ-H2AX foci on SCs even at the highest dose tested (Fig. 5Ba and a′). γ-rays were found to lead to additional L-foci in cells at early and late pachytene, and the number of these foci increased with the received dose from 0.5-2 Gy; it was greater in early (from 2.8- to 5.2-fold) than late (from 1.4- to 3.4-fold) pachytene cells (Fig. 5Ba). We then determined the kinetics of appearance and disappearance of radioinduced γ-H2AX foci at different time-points (from 15 minutes to 26 hours) after irradiation at a dose of 1 Gy (Fig. 5Bb and b′). A ten- to 16-fold increase of L-foci number (12 to 15 additional L-foci) was observed at both early and late pachytene within 15 minutes after irradiation, reached a maximum 1 hour post-irradiation and remained constant for another hour (about 17 to 20 additional L-foci). Four hours after irradiation the number of L-foci had decreased leading to the disappearance of 82.5% of the radioinduced L-foci (14 to 16 L-foci less) by 8 hours after irradiation. The number of L-foci returned to its basal value 18 hours later (Fig. 5Bb). Thus, with a dose of 1 Gy, up to 20 L-foci were rapidly generated (within 15 minutes) in pachytene cells, most likely as a consequence of DSB formation. These foci then disappear within 4-8 hours presumably in parallel with DSB repair.

S-foci were more difficult to detect and measure for two reasons: first, at early time points after irradiation, the relatively high number of L-foci prevented S-foci detection. Second, given the high number of background level of S-foci (i.e. already present in non-irradiated cells), new S-foci could be detected only if they contributed to a statistically significant proportion of total foci. Assays of various doses did not reveal any dose-effect relationship in contrast to L-foci (Fig. 5Ba′) and irradiation at 1 Gy was chosen for further analysis. Counts of S-foci were found to be highly reproducible and irradiation at 1 Gy lead to two waves of increases in S-foci number at both early and late pachytene (Fig. 5Bb′). The first increase was apparent 1 hour or 2 hours post irradiation according to the pachytene stage analyzed (about 12 to 17 additional S-foci). After 4 hours, the number of S-foci decreased to the basal level. A second transient increase in S-foci number was observed 8 hours post irradiation (about 12 to 13 additional S-foci).

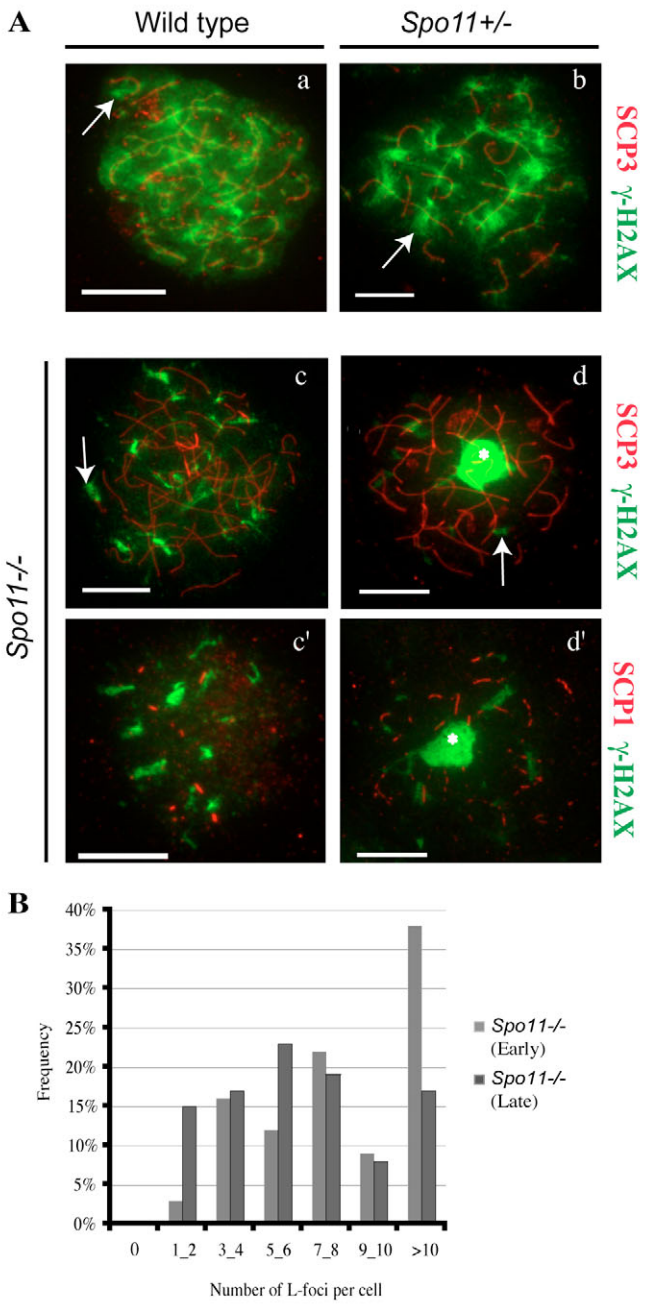

Fig. 3. (A) *Spo11*$^{-/-}$ zygotene cells are devoid of S-foci. In contrast to wild-type (a) and *Spo11*$^{+/-}$ (b) zygotene cells, surface-spread preparations of *Spo11*$^{-/-}$ zygotene cells stained for SCP3 (red) revealed the presence of L-foci and a lack of S-foci on the axial elements (c,d). *Spo11*$^{-/-}$ zygotene cells exhibited γ-H2AX signals that looked like L-foci (c,d). We defined two categories of zygotene *Spo11*$^{-/-}$ cells: (c) without or (d) with a pseudo sex body (*). In c′ and d′, zygotene stages of *Spo11*$^{-/-}$ nuclei were defined by co-labeling of SCP1 (red) and γ-H2AX (green): SCP1-positive nuclei with a pseudo sex body corresponded to the most advanced stage (d′). Arrows indicate L-foci. Bars, 10 μm. (B) Change in the distribution of γ-H2AX L-foci during zygotene stage in *Spo11*$^{-/-}$ mice. Zygotene nuclei from early (light gray bars) and late (dark gray bars) stages were classified according to their number of L-foci. A quantitative analysis of L-foci in *Spo11*$^{-/-}$ zytotenes revealed that the most advanced cells (with a pseudo sex body) contained less L-foci.

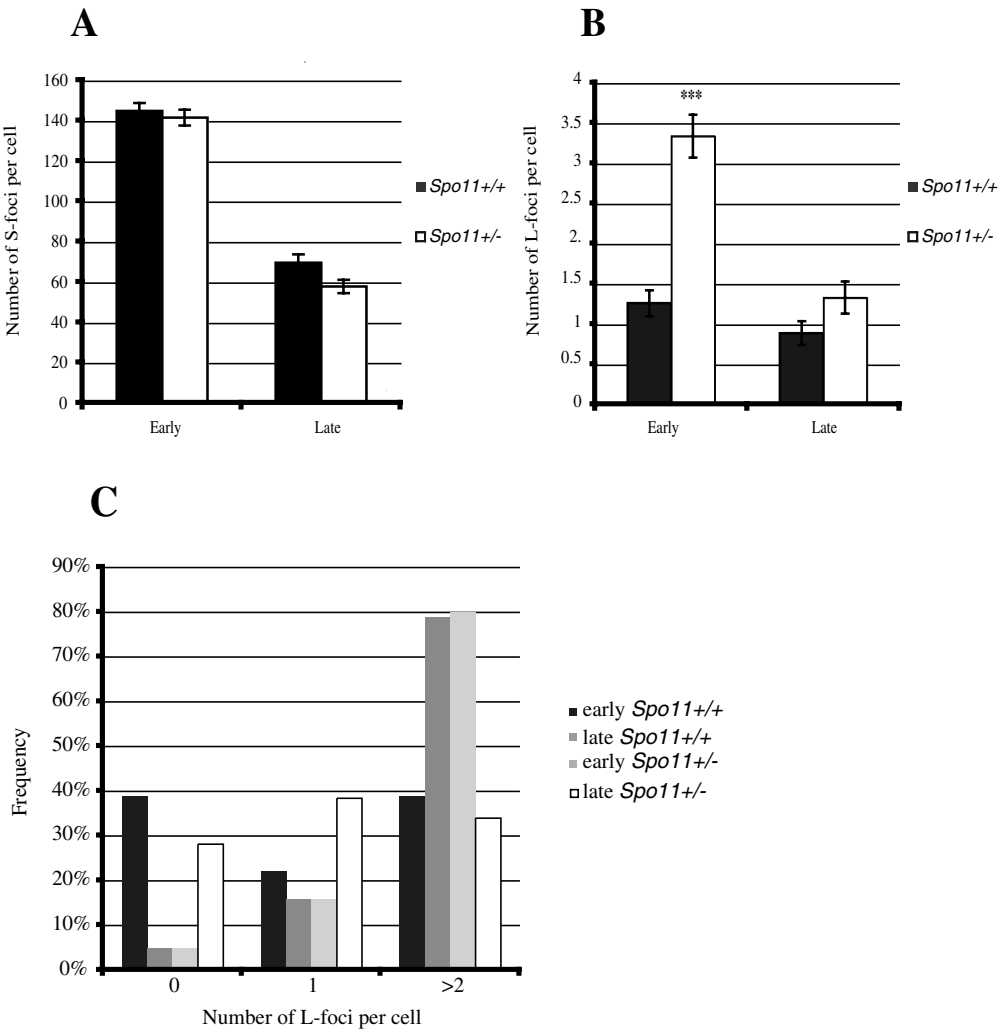

Fig. 4. *Spo11*$^{+/-}$ early pachytene cells exhibit the same number of S-foci but contain more L-foci than *Spo11*$^{+/+}$ early pachytene cells. (A,B) Quantification of γ-H2AX containing S-foci (A) and L-foci (B) in early and late *Spo11*$^{+/+}$ and *Spo11*$^{+/-}$ pachytene cells (black and white bars, respectively). Bars represent mean numbers ±s.e.m. for each experimental group (n=3). Statistical comparisons between *Spo11*$^{+/+}$ and *Spo11*$^{+/-}$ mice at early and late pachytene were performed using the Mann-Whitney U test. Significance is ***P<0.001. (C) Distinct repartition of L-foci in *Spo11*$^{+/-}$ and *Spo11*$^{+/+}$ pachytene spermatocytes. Pachytene nuclei of *Spo11*$^{+/+}$ mice (black and dark gray bars) and *Spo11*$^{+/-}$ mice (light gray and white bars) were classified according to their number of L-foci.

Taken together, this analysis of L- and S-foci formation upon irradiation indicates a major induction of L-foci from 15 minutes to 1 hour after irradiation. Although the variations of S foci number was more difficult to evaluate, the transient increase in S-foci number is compatible with the notion that, upon DSB repair, L-foci are converted into S foci, as suggested by the in vivo meiotic cell analysis. The observation of two waves of S foci formation remains to be understood however (see Discussion).

To further confirm the relationship between L- and S-foci formation and DSB formation and repair in pachytene spermatocytes, we looked at the impact of either neocarzinostatin (NCS) (Noel et al., 2003) described as a specific DSB inducer and MMS (methyl methane sulfonate), assumed to induce single-strand breaks (SSBs) only (Campalans et al., 2005). Because these experiments can only be conducted in vitro, we developed and validated conditions of in vitro maintenance of testicular cells for several hours. Namely we found comparable effects of irradiation in vivo and in vitro (not shown). An increase in the number of L-foci was clearly observed 10 minutes after NCS treatment (Fig. 5Bc), similarly to what was observed 15 minutes after cell irradiation (Fig. 5Bb). The variation in S-foci number was not detected in either early or late pachytene cells (Fig. 5Bc′). Upon MMS treatment no additional L-foci were detected, in agreement with our interpretation of L-foci as mark for DSB formation (Fig. 5Bd).

Discussion

Previous reports have shown that phosphorylation of H2AX during meiotic prophase is first apparent in ‘chromatin domains’ at leptotene until early zygotene, associated with meiotic DSBs (Hunter et al., 2001; Mahadevaiah et al., 2001), and then exclusively on the sex body. Here, we show that two types of γ-H2AX signal appear and coexist from zygotene to diplotene: discreet S-foci along axial and lateral elements of autosomes, and larger L-foci attached to SCs but extending into chromatin loops. Numerous S- and L-foci were detectable from the onset of zygotene, and the number of L-foci declined gradually until becoming a rare event throughout pachytene and diplotene. By contrast, we still found at pachytene multiple S-foci along the SC, as previously described in human and grasshopper (Lenzi et al., 2005; Roig et al., 2004; Viera et al., 2004). Their number progressively decreased from about 120 to 50 from early to late pachytene and finally to zero at diplotene. γ-H2AX S-foci were observed in different mouse strains (NMRI, C57/BL6x129SvJ mixed background and C57/BL6, data not shown) and other rodent species. This study

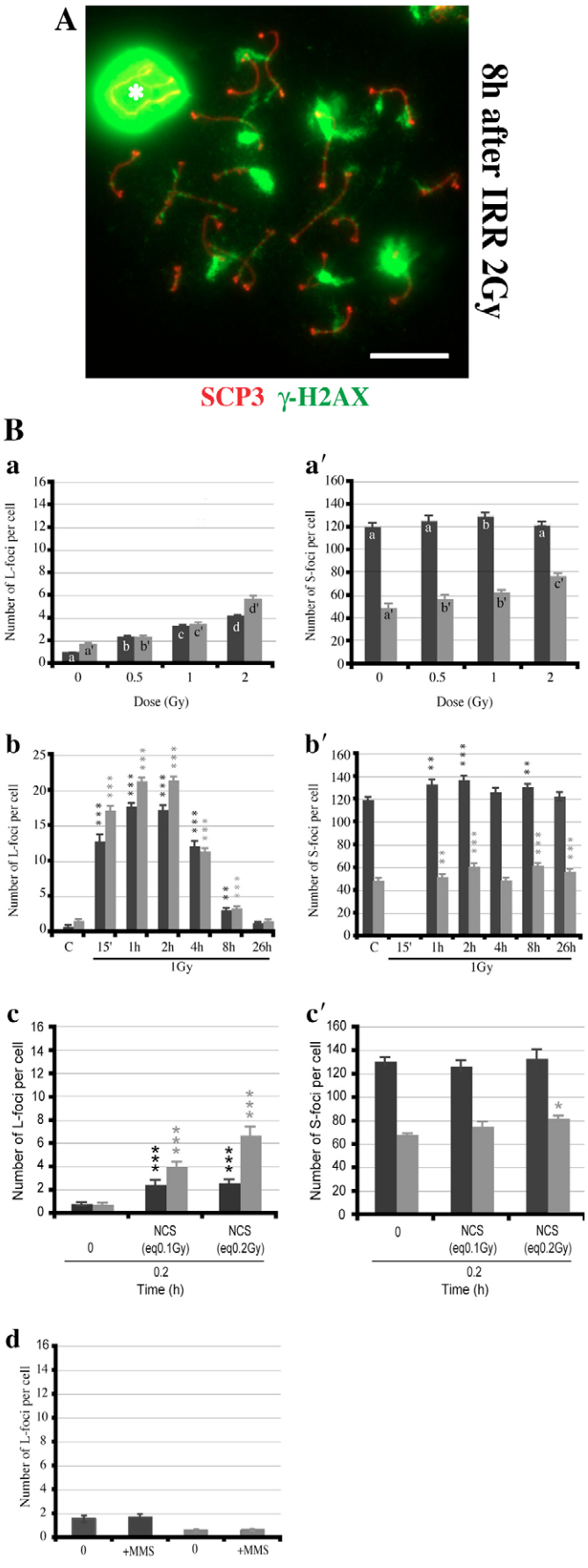

Fig. 5. Induction of both γ-H2AX-containing S-foci and L-foci on late pachytene chromosome spreads 8 hours after irradiation at 2 Gy. (A) Late pachytene cell stained for γ-H2AX (green) and SCP3 (red) reveals additional signals that look like S-foci and L-foci in irradiated cells compared with untreated cells (see Fig. 1Ae). *, XY body. Bar, 10 μm. (B) Effect of increasing doses of γ-rays on γ-H2AX foci number in pachytene cell 8 hours after irradiation. (a,a′) Dose-dependent increase was found in L-foci number (a) but not in S-foci number (a′). Each column represents the mean ±s.e.m. at early (black bars) and late (gray bars) pachytene of at least three independent experiments. Lower case letters correspond to multiple comparisons of mean number of S-foci and L-foci according to the γ-ray doses given at a certain pachytene stage. Lower case letters are different at significantly different *P*-values ($P<0.05$). (b,b′) Time-course of disappearance of γ-H2AX S-foci and L-foci after 1 Gy exposure to γ-irradiation; L-foci (b) and S-foci (b′) mean number ±s.e.m. of at least three independent experiments at early (black bars) and late (gray bars) pachytene. Counting of S-foci could not be done at 15 minutes. Statistical comparisons to the control were performed at a given pachytene stage by using the Student's *t*-test; $^{**}P<0.01$, $^{***}P<0.001$. (c,c′) Concomitant induction of γ-H2AX S-foci and L-foci after treatment with neocarzinostatin in vitro equivalent to a dose of 0.5 Gy; L-foci (c) and S-foci (c′) mean number ±s.e.m. for each experimental group ($n=2$). Statistical comparisons to the control at a given pachytene stage were performed by the Student's *t*-test. $^{*}P<0.05$. (d) MMS cell treatment does not induce γ-H2AX L-foci. Bars represent mean number ± s.e.m. for each experimental group ($n=5$) at early and late pachytene.

focused on disclosing the nature of both S- and L-foci during meiosis.

γ-H2AX S-foci as Spo11-DSB repair

Several lines of evidence support the hypothesis that S-foci detected at zygotene up to late pachytene indicate *Spo11*-induced DSB repair. We found the number of S-foci at early pachytene comparable to those of meiotic DSBs counted at the end of zygotene by Moens et al. (Moens et al., 2002). The progressive disappearance of these foci coincides with the time course of repair of meiotic DSBs (Keogh et al., 2006) and a subset of them colocalize with RAD51/DMC1 and MLH1 foci at early and late pachytene, respectively. Such collocations were also observed in human and grasshopper spermatocytes (Roig et al., 2004; Viera et al., 2004). Finally, in contrast to $Spo11^{+/+}$ and $Spo11^{+/-}$ cells, $Spo11^{-/-}$ zygotene cells were devoid of S-foci. Interestingly, at pachytene, we found that the number of S-foci was the same for $Spo11^{+/+}$ and $Spo11^{+/-}$ mice, in spite of the heterozygote invalidation of *Spo11*. This suggests that the predicted reduction in the number of SPO11-DSBs induced at leptotene was balanced before the pachytene stage. Accordingly, reduced γ-H2AX histone levels were observed in extracts from juvenile $Spo11^{+/-}$ testes (i.e. containing spermatocytes up to leptotene or early zygotene stage), whereas the same number of MLH1 foci was observed at pachytene in $Spo11^{+/-}$ and wild type [F. Cole, M. Jasin and S. Keeney (Molecular Biology Program, Memorial Sloane-Kettering Cancer Center, New York, NY), personal communication]. Thanks to this result, we propose that S-foci indicate chromatin sites of gene conversion events that depend on *Spo11*, including those converted to CRs. At the chromatin level, S-foci might derive from the larger domains of γ-H2AX observed at leptotene around *Spo11*-induced DSB, indicating that a process of histone exchange or modification leads to the loss of the

phosphorylated form of H2AX in two waves, first along the large chromatin domain, leading to S foci, then in the vicinity of the region undergoing DSB repair itself. The first wave might result from an early step of DSB repair (strand invasion, for instance), the second from completion of the DSB repair event.

γ-H2AX L-foci indicate DSBs before completion of DNA repair

This study provided us with several arguments showing that L-foci actually indicate newly formed DSBs at stages preceding DNA repair. Indeed, after treatment of pachytene cells by DSB-inducers (NCS and γ-rays), L-foci were transient: they appeared soon after treatment (10-15 minutes) and then progressively disappeared within a few to several hours. Similar kinetics of successive phosphorylation and dephosphorylation of γ-H2AX have been found in irradiated somatic cells (Gavrilov et al., 2006; Nowak et al., 2006). The observation of a small number of L-foci in untreated pachytene cells is still open to several alternative interpretations. They could clearly mark regions with unrepaired DSBs, formed at leptotene along the wave of *Spo11* DSB induction, which requires ATM (Bellani et al., 2005). It cannot be excluded that these L-foci are induced later by ATM or a yet unknown kinase. Persistence of L-foci until diakinesis suggests that their lifespan is longer than most other γ-H2AX signals, unless a constant activity generates them. Their persistence could alternatively reflect not a defect of DSB repair but an inappropriate removal of γ-H2AX in a region where DSB repair has been completed. One argument, coherent with a problem of DNA repair, comes from the observation of similar foci in an azoospermic man exhibiting a defect in meiotic DSB repair (Sciurano et al., 2006) and also in mice carrying mutations that affect either the repair of DSBs (*Dmc1*, *Msh5*, *Atm*) (Barchi et al., 2005) or SC assembly (*Scyp1*) (de Vries et al., 2005). Furthermore, these γ-H2AX foci were associated with RAD51/DMC1 foci at both pachytene and diplotene in $Atm^{-/-}Spo11^{+/-}$ and $Scyp1^{-/-}$ mice (Bellani et al., 2005; de Vries et al., 2005). The fact that we found differences in the number of L-foci throughout pachytene between $Spo11^{+/-}$ and $Spo11^{+/+}$ is also coherent with a direct link with DSB repair regulated either in terms of schedule (Bellani et al., 2005; de Vries et al., 2005) or by a homeostatic control similar to that described in yeast (Martini et al., 2006).

γ-H2AX L-foci might also point to other modifications in chromosome structure

Additional information on L-foci came from the analysis of $Spo11^{-/-}$ mice. We found that early zygotene cells exhibited more L-foci than late zygotene cells, and γ-H2AX signals were already detected at leptotene (data not shown). At late zygotene or early pachytene stage, most nuclei showed globular γ-H2AX staining corresponding to the pseudo sex body, and a small number to zero L-foci. These foci might be the result from uncharacterized DNA alterations occurring during S phase, or a response to the synapsis failure. A role for Spo11 in meiotic S phase has actually been reported in yeast (Cha et al., 2000). However, given the limited numbers and areas covered by L-foci, it seems clear that the failure to form a synapse is not sufficient. Co-staining with SCP1 did not reveal specific colocalization with L-foci, therefore, nonhomologous synapsis formation is not involved either. Whatever the mechanism responsible for the signal, the pseudo sex body may be the result of the clustering of these domains. γ-H2AX L-foci detected at $Spo11^{-/-}$ zygotene were not labeled by ATR, in contrast to the pseudo sex body previously described by Bellani et al. (Bellani et al., 2005).

In conclusion, we propose that γ-H2AX L-foci reflect the presence of DSB formation and possibly another chromosome alteration present in $Spo11^{-/-}$ cells. S-foci have features that are compatible with sites at with DSB repair takes place. Importantly, our analyses suggest two waves of control potentially linked to monitoring the progression of meiotic prophase – as shown by the two-stage disappearance of γ-H2AX.

Materials and Methods

Animals

Adult NMRI and C57/BL6 strain mice (Charles River Laboratories, l'Arbresle, France), $Spo11^{-/-}$, $Spo11^{+/-}$ and $Spo11^{+/+}$ mice (Baudat et al., 2000) with a mixed C57/BL6x129Sv background were used in this study. Experiments were done under supervision of Ile de France I Ethics Committee and according to French regulations (Ministry of Agriculture Decree 87-848).

Spermatocyte culture

A suspension of testicular cells was prepared using enzymatic digestion with 100 U/ml collagenase type I (Invitrogen) for 25 minutes at 32°C in Hank's balanced salt solution (HBSS) supplemented with 20 mM HEPES (pH 7.2), 1.2 mM $MgSO_4$, 1.3 mM $CaCl_2$, 6.6 mM sodium pyruvate and 0.05% lactate. The resulting cell suspension was filtered through a 40-μm nylon mesh to remove cell clumps. The cell pellet was washed with HBSS and resuspended at the concentration of 1.5×10^6 per ml in MEM-α with glutamax without deoxyribonucleosides and ribonucleosides (Invitrogen) supplemented with 1.2 mM $MgSO_4$, 1.3 mM $CaCl_2$, 6.6 mM sodium pyruvate, 0.05% lactate, 2% bovine serum albumin (BSA), 5% heat-inactivated fetal calf serum and an antibiotic-antimycotic cocktail (Invitrogen), pH 7.1.

Irradiation and chemicals

Mice were whole-body exposed to γ-rays from a 137 Cs source (IBL 637 Cis Bio International, France). Three doses were tested (0.5, 1 and 2 Gy) at a dose rate of 0.63 Gy/minute. For in vitro analyses, testicular cells were irradiated under the same conditions at 1 Gy and maintained for 3-7 hours in culture in the medium described above. For treatment with neocarzinostatin (NCS; kind gift from V. Favaudon, Unité 350 INSERM, Institut Curie-Recherche Bâts 110-112, Centre Universitaire, Orsay, France), NCS was prepared and titrated as described (Favaudon, 1983). Working solutions were prepared immediately before use in ice-cold 1×PBS buffer without $CaCl_2$ and $MgCl_2$ (Invitrogen). Cultured testicular cells were treated for 10 minutes, 3 hours and 7 hours with increasing concentrations of NCS. Because 1 nM NCS yields the same amount of DSBs as 1.21 Gy γ-rays (Noel et al., 2003), we treated the cells at concentrations equivalent to 0.1, 0.2 and 0.5 Gy.

Spermatocyte chromosome preparations

Two types of spermatocyte chromosome preparation were made, depending on protein labeling, for all rodent species studied. For γ-H2AX and MLH1 immunodetection, chromosomes were prepared according to the drying-down technique of Peters et al. (Peters et al., 1997) with some minor modifications. Tubules were minced in hypotonic extraction buffer for 50 minutes. The supernatant was then centrifuged for 5 minutes at 1200 rpm in a table-top centrifuge, the cell suspension volume was adjusted and the cells were fixed using 1% paraformaldehyde containing 0.2% Triton X-100. Colocalization of RAD51/DMC1 foci together with SCs containing γ-H2AX foci was performed on spermatocytes surface-spread on 0.1 M NaCl, attached to glass slides, fixed in 1% paraformaldehyde at 4°C, and washed in Photo-Flo 200 (Sigma).

MMS cell treatment

Spermatocytes were treated at room temperature with 0.5 mM MMS (Sigma) during the last 20 minutes of hypotonic shock. Cells were then rinsed and fixed at 4°C within the 15 minutes to induce single-strand breaks (SSB).

Antibodies

Primary antibodies used in this study were polyclonal rabbit anti-SCP3 (kind gift from C. Heyting; 1:1000 dilution), polyclonal guinea pig anti-SCP3 (Peptide Specialty Laboratories GmbH; 1:100 dilution), polyclonal goat anti-ATR protein (Santa-cruz Biotechnology; 1:200 dilution), polyclonal rabbit anti-RAD51 that crossreact with DMC1 proteins (Pharmingen-BD Biosciences; 1:40 dilution), polyclonal rabbit and monoclonal mouse anti-γ-H2AX (Upstate; 1:200 dilution), monoclonal mouse anti-human MLH1 (Pharmingen-BD Biosciences; 1:50 dilution).

Secondary antibodies were:
donkey anti-rabbit cyanin 3 (Jackson ImmunoResearch; 1:400 dilution);
donkey anti-rabbit fluorescein (Jackson ImmunoResearch; 1:100 dilution);
donkey anti-rabbit cyanin 5 (Jackson ImmunoResearch; 1:50 dilution);
donkey anti-rabbit antibody fluorescein (Jackson ImmunoResearch; 1:100 dilution);
donkey anti-mouse fluorescein (Jackson ImmunoResearch; 1:50 dilution);
donkey anti-guinea-pig cyanin 3 (Jackson ImmunoResearch; 1:400 dilution).

Immunofluorescence

Spermatocyte preparations were blocked in PBT (1% BSA, 3% SVF, 0,05% Triton X-100) for 30 minutes. For XRCC1 labeling, previous washes in Photo-flo 200 0,4%/H_2O (Sigma, Saint Quentin Fallavier, France) were performed and slides were air-dried at least 15 minutes before blocking. Slides were then incubated with primary antibodies diluted in PBT for 1 hour at 37°C. After several PBS washes, appropriate secondary antibodies were incubated for 1 hour at 37°C and slides were washed with PBS, and then mounted with Vectashield (Vector Laboratories). RAD51/DMC1 immunolabeling was performed as described in Kwan et al. (Kwan et al., 2003). For in vivo experiment at least 30 cells were analyzed per animal. For in vitro cell preparations, pooled of testis from two animals were used and at least 30 cells were analyzed per condition.

Spermatocyte staging

In all rodent species, the stages of meiotic prophase were identified using antibodies directed against protein SCP3, a component of axial element precursors of the lateral elements of the SCs following the criteria described by Moses (Moses, 1980).

Microscopy

Image capture and analysis were performed using an Olympus AX70 epifluorescent microscope equipped with a charge-coupled camera (Roper Scientific) and IPlab software (Scanalytics). An IPlab software tool was used to measure SC lengths. Adobe Photoshop 7.0 software (Adobe Systems Incorporated) was used for image processing.

Data analysis

Each point represents the mean ± s.e.m. (standard error of the mean) of at least three independent experiments. Data were analyzed by one-way ANOVA followed by the Tukey-Kramer multiple corrections test, the Mann-Whitney U test (Graphpad Instat 3.0 software) or the χ^2 test (χ^2, υ=degrees of freedom–1; Statview Software).

This work was supported by Electricité de France (EDF) to B.D. and by the Association pour la Recherche contre le Cancer (contract 3723) to B.deM. We thank P. Radicella, A. Campalans for providing MMS and XRCC1 antibodies and useful advice, F. Baudat for mouse genotyping and discussions, and F. Fabre for critical reading of manuscript. We are grateful to V. Favaudon for providing neocarzinostatin.

References

Allers, T. and Lichten, M. (2001). Differential timing and control of noncrossover and crossover recombination during meiosis. *Cell* **106**, 47-57.
Anderson, L. K., Reeves, A., Webb, L. M. and Ashley, T. (1999). Distribution of crossing over on mouse synaptonemal complexes using immunofluorescent localization of MLH1 protein. *Genetics* **151**, 1569-1579.
Antonelli, F., Belli, M., Cuttone, G., Dini, V., Esposito, G., Simone, G., Sorrentino, E. and Tabocchini, M. A. (2005). Induction and repair of DNA double-strand breaks in human cells: dephosphorylation of histone H2AX and its inhibition by calyculin A. *Radiat. Res.* **164**, 514-517.
Ashley, T., Plug, A. W., Xu, J., Solari, A. J., Reddy, G., Golub, E. I. and Ward, D. C. (1995). Dynamic changes in Rad51 distribution on chromatin during meiosis in male and female vertebrates. *Chromosoma* **104**, 19-28.
Ashley, T., Gaeth, A. P., Creemers, L. B., Hack, A. M. and De Rooij, D. G. (2004). Correlation of meiotic events in testis sections and microspreads of mouse spermatocytes relative to the mid-pachytene checkpoint. *Chromosoma* **113**, 126-136.
Baarends, W. M., Wassenaar, E., van der Laan, R., Hoogerbrugge, J., Sleddens-Linkels, E., Hoeijmakers, J. H., de Boer, P. and Grootegoed, J. A. (2005). Silencing of unrepaired chromatin and histone H2A ubuquitination in mammalian meiosis. *Mol. Cell Biol.* **25**, 1041-1053.
Baart, E. B., de Rooij, D. G., Keegan, K. S. and de Boer, P. (2000). Distribution of Atr protein in primary spermatocytes of a mouse chromosomal mutant: a comparison of preparation techniques. *Chromosoma* **109**, 139-147.
Baker, S. M., Plug, A. W., Prolla, T. A., Bronner, C. E., Harris, A. C., Yao, X., Christie, D. M., Monell, C., Arnheim, N. and Bradley, A. (1996). Involvement of mouse Mlh1 in DNA mismatch repair and meiotic crossing over. *Nat. Genet.* **13**, 336-342.
Barchi, M., Mahadevaiah, S., Di Giacomo, M., Baudat, F., de Rooij, D. G., Burgoyne, P. S., Jasin, M. and Keeney, S. (2005). Surveillance of different recombination defects in mouse spermatocytes yields distinct responses despite elimination at an identical developmental stage. *Mol. Cell. Biol.* **25**, 7203-7215.
Barlow, A. L., Benson, F. E., West, S. C. and Hulten, M. A. (1997). Distribution of the Rad51 recombinase in human and mouse spermatocytes. *EMBO J.* **16**, 5207-5215.
Bassing, C. H. and Alt, F. W. (2004). The cellular response to general and programmed DNA double strand breaks. *DNA Repair Amst.* **3**, 781-796.
Baudat, F. and Keeney, S. (2001). Meiotic recombination: making and breaking go hand in hand. *Curr. Biol.* **11**, R45-R48.
Baudat, F., Manova, K., Yuen, J. P., Jasin, M. and Keeney, S. (2000). Chromosome synapsis defects and sexually dimorphic meiotic progression in mice lacking Spo11. *Mol. Cell* **6**, 989-998.
Bellani, M. A., Romanienko, P. J., Cairatti, D. A. and Camerini-Otero, R. D. (2005). SPO11 is required for sex-body formation, and Spo11 heterozygosity rescues the prophase arrest of Atm–/– spermatocytes. *J. Cell Sci.* **118**, 3233-3245.
Borner, G. V., Kleckner, N. and Hunter, N. (2004). Crossover/noncrossover differentiation, synaptonemal complex formation, and regulatory surveillance at the leptotene/zygotene transition of meiosis. *Cell* **117**, 29-45.
Bouquet, F., Muller, C. and Salles, B. (2006). The loss of gammaH2AX signal is a marker of DNA double strand breaks repair only at low levels of DNA damage. *Cell Cycle* **5**, 1116-1122.
Campalans, A., Marsin, S., Nakabeppu, Y., O'Connor, T. R., Boiteux, S. and Radicella, J. P. (2005). XRCC1 interactions with multiple DNA glycosylases: a model for its recruitment to base excision repair. *DNA Repair Amst.* **4**, 826-835.
Cha, R. S., Weiner, B. M., Keeney, S., Dekker, J. and Kleckner, N. (2000). Progression of meiotic DNA replication is modulated by interchromosomal interaction proteins, negatively by Spo11p and positively by Rec8p. *Genes Dev.* **14**, 493-503.
de los Santos, T., Hunter, N., Lee, C., Larkin, B., Loidl, J. and Hollingsworth, N. M. (2003). The Mus81/Mms4 endonuclease acts independently of double-Holliday junction resolution to promote a distinct subset of crossovers during meiosis in budding yeast. *Genetics* **164**, 81-94.
de Vries, F. A., de Boer, E., van den Bosch, M., Baarends, W. M., Ooms, M., Yuan, L., Liu, J. G., van Zeeland, A. A., Heyting, C. and Pastink, A. (2005). Mouse Sycp1 functions in synaptonemal complex assembly, meiotic recombination, and XY body formation. *Genes Dev.* **19**, 1376-1389.
Favaudon, V. (1983). Gamma-radiolysis study of the reductive activation of neocarzinostatin by the carboxyl radical. *Biochimie* **65**, 593-607.
Fernandez-Capetillo, O., Lee, A., Nussenzweig, M. and Nussenzweig, A. (2004). H2AX: the histone guardian of the genome. *DNA Repair Amst.* **3**, 959-967.
Forand, A., Dutrillaux, B. and Bernardino-Sgherri, J. (2004). Gamma-H2AX expression pattern in non-irradiated neonatal mouse germ cells and after low-dose gamma-radiation: relationships between chromatid breaks and DNA double-strand breaks. *Biol. Reprod.* **71**, 643-649.
Gavrilov, B., Vezhenkova, I., Firsanov, D., Solovjeva, L., Svetlova, M., Mikhailov, V. and Tomilin, N. (2006). Slow elimination of phosphorylated histone gamma-H2AX from DNA of terminally differentiated mouse heart cells in situ. *Biochem. Biophys. Res. Commun.* **347**, 1048-1052.
Guillon, H. and de Massy, B. (2002). An initiation site for meiotic crossing-over and gene conversion in the mouse. *Nat. Genet.* **32**, 296-299.
Hunter, N., Borner, G. V., Lichten, M. and Kleckner, N. (2001). Gamma-H2AX illuminates meiosis. *Nat. Genet.* **27**, 236-238.
Keogh, M. C., Kim, J. A., Downey, M., Fillingham, J., Chowdhury, D., Harrison, J. C., Onishi, M., Datta, N., Galicia, S. and Emili, A. (2006). A phosphatase complex that dephosphorylates gammaH2AX regulates DNA damage checkpoint recovery. *Nature* **439**, 497-501.
Kwan, K. Y., Moens, P. B. and Wang, J. C. (2003). Infertility and aneuploidy in mice lacking a type IA DNA topoisomerase III beta. *Proc. Natl. Acad. Sci. USA* **100**, 2526-2531.
Lenzi, M. L., Smith, J., Snowden, T., Kim, M., Fishel, R., Poulos, B. K. and Cohen, P. E. (2005). Extreme heterogeneity in the molecular events leading to the establishment of chiasmata during meiosis i in human oocytes. *Am. J. Hum. Genet.* **76**, 112-127.
Lipkin, S. M., Moens, P. B., Wang, V., Lenzi, M., Shanmugarajah, D., Gilgeous, A., Thomas, J., Cheng, J., Touchman, J. W. and Green, E. D. (2002). Meiotic arrest and aneuploidy in MLH3-deficient mice. *Nat. Genet.* **31**, 385-390.
MacPhail, S. H., Banath, J. P., Yu, T. Y., Chu, E. H., Lambur, H. and Olive, P. L. (2003). Expression of phosphorylated histone H2AX in cultured cell lines following exposure to X-rays. *Int. J. Radiat. Biol.* **79**, 351-358.
Mahadevaiah, S. K., Turner, J. M., Baudat, F., Rogakou, E. P., de Boer, P., Blanco-Rodriguez, J., Jasin, M., Keeney, S., Bonner, W. M. and Burgoyne, P. S. (2001). Recombinational DNA double-strand breaks in mice precede synapsis. *Nat. Genet.* **27**, 271-276.
Marcon, E. and Moens, P. (2003). MLH1p and MLH3p localize to precociously induced chiasmata of okadaic-acid-treated mouse spermatocytes. *Genetics* **165**, 2283-2287.
Martini, E., Diaz, R. L., Hunter, N. and Keeney, S. (2006). Crossover homeostasis in yeast meiosis. *Cell* **126**, 285-295.
Moens, P. B., Chen, D. J., Shen, Z., Kolas, N., Tarsounas, M., Heng, H. H. and Spyropoulos, B. (1997). Rad51 immunocytology in rat and mouse spermatocytes and oocytes. *Chromosoma* **106**, 207-215.
Moens, P. B., Kolas, N. K., Tarsounas, M., Marcon, E., Cohen, P. E. and Spyropoulos, B. (2002). The time course and chromosomal localization of recombination-related proteins at meiosis in the mouse are compatible with models that can resolve the early DNA-DNA interactions without reciprocal recombination. *J. Cell Sci.* **115**, 1611-1622.
Moses, M. J. (1980). *New Cytogenetics Studies on Mammalian Meiosis*. New York: Raven.

Nagata, T., Kato, T., Morita, T., Nozaki, M., Kubota, H., Yagi, H. and Matsushiro, A. (1991). Polyadenylated and 3′ processed mRNAs are transcribed from the mouse histone H2A.X gene. *Nucleic Acids Res*. **19**, 2441-2447.

Nazarov, I. B., Smirnova, A. N., Krutilina, R. I., Svetlova, M. P., Solovjeva, L. V., Nikiforov, A. A., Oei, S. L., Zalenskaya, I. A., Yau, P. M. and Bradbury, E. M. (2003). Dephosphorylation of histone gamma-H2AX during repair of DNA double-strand breaks in mammalian cells and its inhibition by calyculin A. *Radiat. Res*. **160**, 309-317.

Neyton, S., Lespinasse, F., Moens, P. B., Paul, R., Gaudray, P., Paquis-Flucklinger, V. and Santucci-Darmanin, S. (2004). Association between MSH4 (MutS homologue 4) and the DNA strand-exchange RAD51 and DMC1 proteins during mammalian meiosis. *Mol. Hum. Reprod*. **10**, 917-924.

Noel, G., Giocanti, N., Fernet, M., Megnin-Chanet, F. and Favaudon, V. (2003). Poly(ADP-ribose) polymerase (PARP-1) is not involved in DNA double-strand break recovery. *BMC Cell Biol*. **4**, 7.

Nowak, E., Etienne, O., Millet, P., Lages, C. S., Mathieu, C., Mouthon, M. A. and Boussin, F. D. (2006). Radiation-induced H2AX phosphorylation and neural precursor apoptosis in the developing brain of mice. *Radiat. Res*. **165**, 155-164.

Paull, T. T., Rogakou, E. P., Yamazaki, V., Kirchgessner, C. U., Gellert, M. and Bonner, W. M. (2000). A critical role for histone H2AX in recruitment of repair factors to nuclear foci after DNA damage. *Curr. Biol*. **10**, 886-895.

Peters, A. H., Plug, A. W., van Vugt, M. J. and de Boer, P. (1997). A drying-down technique for the spreading of mammalian meiocytes from the male and female germline. *Chromosome Res*. **5**, 66-68.

Peterson, C. L. and Cote, J. (2004). Cellular machineries for chromosomal DNA repair. *Genes Dev*. **18**, 602-616.

Redon, C., Pilch, D., Rogakou, E., Sedelnikova, O., Newrock, K. and Bonner, W. (2002). Histone H2A variants H2AX and H2AZ. *Curr. Opin. Genet. Dev*. **12**, 162-169.

Rogakou, E. P., Pilch, D. R., Orr, A. H., Ivanova, V. S. and Bonner, W. M. (1998). DNA double-stranded breaks induce histone H2AX phosphorylation on serine 139. *J. Biol. Chem*. **273**, 5858-5868.

Rogakou, E. P., Boon, C., Redon, C. and Bonner, W. M. (1999). Megabase chromatin domains involved in DNA double-strand breaks in vivo. *J. Cell Biol*. **146**, 905-916.

Roig, I., Liebe, B., Egozcue, J., Cabero, L., Garcia, M. and Scherthan, H. (2004). Female-specific features of recombinational double-stranded DNA repair in relation to synapsis and telomere dynamics in human oocytes. *Chromosoma* **113**, 22-33.

Romanienko, P. J. and Camerini-Otero, R. D. (2000). The mouse Spo11 gene is required for meiotic chromosome synapsis. *Mol. Cell* **6**, 975-987.

Rothkamm, K. and Lobrich, M. (2003). Evidence for a lack of DNA double-strand break repair in human cells exposed to very low x-ray doses. *Proc. Natl. Acad. Sci. USA* **100**, 5057-5062.

Sciurano, R. B., Rahn, M. I., Pigozzi, M. I., Olmedo, S. B. and Solari, A. J. (2006). An azoospermic man with a double-strand DNA break-processing deficiency in the spermatocyte nuclei: case report. *Hum. Reprod*. **21**, 1194-1203.

Sedelnikova, O. A., Rogakou, E. P., Panyutin, I. G. and Bonner, W. M. (2002). Quantitative detection of (125)IdU-induced DNA double-strand breaks with gamma-H2AX antibody. *Radiat. Res*. **158**, 486-492.

Szostak, J. W., Orr-Weaver, T. L., Rothstein, R. J. and Stahl, F. W. (1983). The double-strand-break repair model for recombination. *Cell* **33**, 25-35.

Tadokoro, Y., Yomogida, K., Yagura, Y., Yamada, S., Okabe, M. and Nishimune, Y. (2003). Characterization of histone H2A.X expression in testis and specific labeling of germ cells at the commitment stage of meiosis with histone H2A.X promoter-enhanced green fluorescent protein transgene. *Biol. Reprod*. **69**, 1325-1329.

Tarsounas, M., Morita, T., Pearlman, R. E. and Moens, P. B. (1999). RAD51 and DMC1 form mixed complexes associated with mouse meiotic chromosome cores and synaptonemal complexes. *J. Cell Biol*. **147**, 207-220.

Thiriet, C. and Hayes, J. J. (2005). Chromatin in need of a fix: phosphorylation of H2AX connects chromatin to DNA repair. *Mol. Cell* **18**, 617-622.

Turner, J. M., Aprelikova, O., Xu, X., Wang, R., Kim, S., Chandramouli, G. V., Barrett, J. C., Burgoyne, P. S. and Deng, C. X. (2004). BRCA1, histone H2AX phosphorylation, and male meiotic sex chromosome inactivation. *Curr. Biol*. **14**, 2135-2142.

Turner, J. M., Mahadevaiah, S. K., Fernandez-Capetillo, O., Nussenzweig, A., Xu, X., Deng, C. X. and Burgoyne, P. S. (2005). Silencing of unsynapsed meiotic chromosomes in the mouse. *Nat. Genet*. **37**, 41-47.

Viera, A., Santos, J. L., Page, J., Parra, M. T., Calvente, A., Cifuentes, M., Gomez, R., Lira, R., Suja, J. A. and Rufas, J. S. (2004). DNA double-strand breaks, recombination and synapsis: the timing of meiosis differs in grasshoppers and flies. *EMBO Rep*. **5**, 385-391.

Yoshida, K., Yoshida, S. H., Shimoda, C. and Morita, T. (2003). Expression and radiation-induced phosphorylation of histone H2AX in mammalian cells. *J. Radiat. Res*. **44**, 47-51.